Numerical Analysis of Variable Property Heat Transfer to a Single Sphere in High Temperature Surroundings

N. N. SAYEGH

and

W. H. GAUVIN

Department of Chemical Engineering
McGill University
Montreal, Quebec, Canada

A theoretical study has been conducted to investigate the effects of large temperature differences on the rate of pure heat transfer from a very hot gas to stationary spheres.

In the numerical analysis, the momentum and energy equations for variable property flow past a sphere were solved simultaneously, using finite difference techniques. Results were obtained for Reynolds numbers up to 50 and surface temperature to gas temperature ratios varying between 0.25 and unity. These ranges cover most of the conditions commonly encountered in heterogeneous plasmas, transferred arc, and other high temperature chemical engineering processes. The flow behavior, drag coefficients, and Nusselt number were calculated for each case.

The constant property solutions were in excellent agreement with numerical and experimental results reported in the literature, thus justifying the validity of the model and of the underlying assumptions. In general, the effect of variable properties was to drastically increase the flow velocity, vorticity, and temperature and vorticity gradients near the surface.

A generalized heat transfer correlation was derived which, in addition to constant property conditions, included the effect of large variations in the physical properties of the fluid as a result of large temperature differences.

SCOPE

The present study forms part of a continuing program of investigation carried out in this laboratory by the Plasma Technology Group towards the application of plasmas to chemical and metallurgical processes of industrial interest. Heterogeneous solids-gas reactions involving the contacting of fine particles with an entraining plasma gas appear to be particularly promising, as for example in the production of such refractory metals as molybdenum, zirconium, and titanium from their respective ores or concentrates, as well as in the production of ferroalloys, such as ferrovanadium and ferrocollumbium. Owing to the very short contacting times available between the high temperature plasma and the entrained particles (of the order of a few milliseconds), an accurate knowledge of the rate of heat transfer to the particles is a prime requirement for the reliable design, operation, and optimization of plasma reactors, particularly when a high degree of conversion is required. The purpose of the present study was to provide this fundamental information.

Although a good deal of work has been published on heat transfer to particles under conditions of moderate temperature difference, little information is available on the situation where this difference is so large that the assumption of constant property flow is no longer permissible. In most heterogeneous plasma systems, the temperature of the particle may range from 1 500° to 2 500°K, while that of the surrounding plasma extends from 5 000°K upward. In addition, the Reynolds number of a particle exposed to a plasma flame is characteristically small, typically less than 50, owing to the unusually high value of the kinematic viscosity.

Needless to say, the findings of this study will also find applications in an ever increasing number of nonplasma, high temperature chemical or metallurgical processes where very large temperature differences exist between the solid and gaseous phases in contact.

The analysis presented in this study is based on the numerical solution of the equations of motion and energy for pure steady state heat transfer and variable property flow at low Reynolds numbers, using finite-difference approximations, thus reducing the nonlinear partial differential equations to a set of nonlinear algebraic equations, which are then solved by iterative methods. Owing to the complexity of the equations involved in this study and to the number of iterations required to reach convergence, considerable attention was devoted to the selection of appropriate mesh size and values of the relaxation coefficient.

N. N. Sayegh is with Pulp and Paper Research Institute of Canada, Pointe Claire, Quebec, Canada. W. H. Gauvin is with Noranda Research Centre, Pointe Claire, Quebec, Canada.

0001-1541-79-2599-0522-$01.55.

CONCLUSIONS AND SIGNIFICANCE

1. Numerical solutions have been obtained for the coupled momentum and energy equations for variable property flow past a sphere. The constant property solutions were generally in excellent agreement with numerical and experimental results reported in the literature. No such comparison was possible for the variable property case, owing to the unavailability of pertinent data.

2. Convergence became more difficult as the Reynolds number or the temperature difference was increased. Very low relaxation coefficient had to be used, thus increasing computation time significantly. This limited the present analysis to $N_{Re} \leq 50$ and dimensionless surface temperature $T_0 \geq 0.25$. T_0 is defined as the ratio of the temperature of the sphere surface to that of the surrounding gas stream.

3. In general, the effect of variable properties was to drastically increase the flow velocity, vorticity, and temperature and vorticity gradients near the surface. The Nusselt number and the drag coefficients were decreased as a result of lower thermal conductivity and viscosity near the surface.

4. The flow separation and the size of the vortex were not markedly affected by the change in the surface temperature. However, as the surface temperature was decreased, the surface pressure was drastically changed, leading in some instances to negative values of the pressure drag coefficient.

5. A general heat transfer correlation has been derived that applies equally to constant and variable property flows. The variations in the fluid properties were accounted for by choosing suitable reference temperatures for the kinematic viscosity and thermal conductivity and by introducing the variable property limiting Nusselt number $2f_0$ to replace the limiting Nusselt number of 2 in the constant property correlation. This equation can be written as

$$N_{Nu_0} = 2f_0 + 0.473\, N_{Pr}^{m} N_{Re_{0.19}}^{0.552}$$

where

$$m = 0.78\, N_{Re_{0.19}}^{-0.145}$$

$$2f_0 = 2(1 - T_0^{1+x})/[(1 + x)(1 - T_0)T_0^{x}]$$

$$= \text{limiting } N_{Nu}$$

$$N_{Re_{0.19}} = UD/\nu_{0.19}$$

In the above, x is the value of the exponent on T, in the expressions relating the viscosity and the thermal conductivity to the absolute temperature. The reference temperature for k is the sphere temperature, and that for ν is $T_{0.19} = T_s + 0.19(T_\infty - T_s)$. Thus, the Nusselt number (and hence the heat transfer coefficient h) are evaluated at the sphere surface temperature, while the Reynolds number (and m) are at $T_{0.19}$.

Use of the mean film temperature resulted in errors in the Nusselt number as high as 20%. The applicability of these reference temperatures for gases having values of x other than that of 0.8 was not, however, verified.

6. The change in the drag coefficient due to positive pressure gradient over the sphere surface cannot be predicted from the constant property situation, and, therefore, the use of average temperatures to correct for varying properties can lead to highly erroneous results.

A large number of studies have been published in the literature on the subject of momentum and heat transport to spheres and cylinders. Clift et al. (1978) give an extensive coverage of transport phenomena around solid and fluid spheres. The review in this section will, therefore, be limited to studies pertinent to the type of flow encountered in plasma jets, transferred electric arcs, and similar high temperature devices and processes, which lie mainly in the low and intermediate ranges of the Reynolds number ($0 < Re < 100$). Also, the emphasis will be more on theoretical analyses of the problems of flow and heat transfer to spheres than on experimental results on drag coefficients or heat transfer rate. An experimental study of the rate of heat transfer to a stationary sphere from an argon, which confirms the present findings, will be presented in a subsequent paper.

FLOW AROUND A SINGLE SPHERE

The Navier-Stokes equations for the flow around a sphere are highly nonlinear, even for the simplified case of constant physical property fluids. Consequently, no completely exact solution exists for these equations.

Following the pioneering work of Stokes (1850) and Oseen (1910), the next significant step was taken by Proudman and Pearson (1957) who obtained higher order approximations for the flow around a sphere by the method of matched asymptotic expansions. These authors used the solutions of Stokes and Oseen as the inner and outer expansions, respectively. By matching these expansions, a uniformly valid asymptotic representation of the flow could be found. In other words, the Proudman and Pearson's solution makes use of the fact that the Stokes' solution is valid near the surface, while Oseen's solution satisfies the flow conditions at large distances away from the sphere. Their analysis was extended by Chester and Breach (1969), following the same method, resulting in a solution which was accurate to a Reynolds number of about 5.

Kawaguti (1955, 1958) obtained separate approximate solutions of the Navier-Stokes equation for the low (0 to 10) and intermediate (10 to 80) ranges of the Reynolds number. He used a Galerkin error-distribution method which involves the choice of a trial polynomial for the stream function that is made to satisfy the flow equations and the boundary conditions. This method was extended by Hamielec et al. (1962, 1963) to viscous flow around fluid and solid spheres at Reynolds numbers up to several thousands. Hoffman and Ross (1972) employed the error-distribution method, modified to include a finite radial mass efflux from the surface, to investigate the effect of mass transfer on heat transfer to

an evaporating droplet.

The earliest finite-difference solution was reported by Jenson (1959) for steady state flow at N_{Re} of 5, 10, 20, and 40. Hamielec et al. (1967) obtained more accurate results by using a finer grid and a larger size field. The Reynolds number range of their solution was between 0.1 and 100. LeClair et al. (1970) extended this work up to N_{Re} of 400. At low N_{Re}, their results departed significantly from those of Jenson while agreeing well with the results of Hamielec and of Rimon and Cheng (1969) at higher N_{Re}. A more thorough discussion of the numerical results was presented by Pruppacher, LeClair, and Hamielec (1970). Rimon and Cheng (1969) solved the time-dependent Navier-Stokes equations numerically for very long times to obtain the steady state solution. LeClair and Hamielec (1970) studied the flow behavior of an accelerating sphere in a viscous fluid in the Reynolds number range of 0.1 to 150. The complete Navier-Stokes equations were solved numerically together with the Basset equation for the sphere.

Dennis and Walker (1971) solved the Navier-Stokes equations for the flow around a sphere for Reynolds numbers between 0.1 and 40. They used a semianalytical formulation where the flow variables were expanded as series of Legendre functions, hence reducing the equations of motion to ordinary differential equations, which were then solved numerically.

All the solutions discussed above were obtained for the case of a constant property fluid. Very few researchers have studied the problem of variable property flow. Kassoy et al. (1966) presented solutions of the momentum equation for cases involving significant variations of the physical properties and temperature. The method of matched asymptotic expansions was used, thus restricting the Reynolds number to the order of unity and the dimensionless temperature difference to the order of the Reynolds number. Seymour (1971) calculated the aerodynamic drag on a small sphere moving in an ionized gas where the temperature ratios between the bulk of the gas and the sphere surface were of the order of 40:1, at $N_{Re} < 1.5$. The properties were allowed to vary exponentially with the temperature.

Woo (1970), using relaxation methods, solved the flow and energy equations numerically for a variable density fluid. The viscosity and the thermal conductivity were assumed temperature independent. Flow patterns were calculated for cases where natural convection was significant. Dumargue et al. (1974) studied the problem of evaporation from a spherical superrefractory particle in a fluid with variable physical properties. The case of zero Reynolds number was solved first. Dufour effects, radiation, and forced convection heat transfer were introduced later by the use of perturbation techniques, while assuming the flow to be Stokesian.

HEAT TRANSFER TO SPHERES

Most of the significant theoretical studies in this field are of rather recent origin. Baird and Hamielec (1962) predicted theoretically approximate local and overall Sherwood numbers for forced convective transfer around solid and fluid spheres for N_{Re} up to 100. The diffusion equation was solved analytically for the case of a thin concentration boundary layer ($N_{Pe} >> 1$). The velocity field used was that derived by Kawaguti and by Hamielec. The results agreed reasonably with experimental correlations of Griffith (1960) and of Ranz and Marshall (1952). Hoffman and Ross (1972), assuming a similar velocity profile, solved the energy equation to investigate the effect of mass transfer on heat transfer. The solution was based on the integral boundary-layer formulation of the energy equation. Solutions were obtained for the case of zero mass efflux in the Prandtl number range of 0.7 to 10 and Reynolds number between 20 and 500.

Series truncation method was used by Dennis, Walker, and Hudson (1973) to solve the energy equation around a sphere. The velocity profiles were those calculated by Dennis and Walker (1971). The basis of the method is to approximate the solution, which in theory consists of an infinite series, by a finite number of terms. For the case of low N_{Re} and N_{Pr} of the order of unity, only few terms are required to give an adequate representation of the flow conditions, making this approach superior to the finite-difference method.

Acrivos and Taylor (1962) solved the equation of energy for the flow around a sphere by the method of matched asymptotic expansions. The flow field used was that given by Stokes' solution. The expression derived was accurate for $N_{Pe} < 1$ and $N_{Re} << 1$. Rimmer (1968) modified this analysis by using the velocity field equations given by Proudman and Pearson (1957). He obtained an expression which was similar to the one given by Acrivos and Taylor, except that it contained one term that was a function of the Prandtl number only.

Assuming the same flow field as that used by Rimmer, Gupalo and Ryazantsev (1972) obtained a solution for the problem of steady state heat or mass transfer when a first-order chemical reaction on the surface of sphere is also considered. Even though the same method of analysis was employed, their results, reduced for the case when the chemical reaction does not influence the transfer process, were different from those of Rimmer for pure heat transfer. These authors claim that certain mistakes in the matching procedure prevented Rimmer from obtaining the correct results.

Kassoy et al. (1966) studied low Reynolds number flow past a sphere for cases involving variations in the fluid properties. The equations of the flow were solved simultaneously with the energy equation, using the method of matched asymptotic expansions. The viscosity and thermal conductivity were allowed to vary linearly with the dimensionless temperature difference. Expressions were given for the Nusselt number, drag coefficient and the pressure distribution.

Woo (1970, 1971) solved the energy equation numerically in conjunction with the equations of the flow. The steady state equations were transformed to difference form using Taylor series expansions (finite-difference method). For the case of forced convection alone, the flow equations were solved first, and the results were then inserted in the energy equation. When natural convection effects were also considered, the density was temperature dependent, and, therefore, both equations had to be solved simultaneously. Local and average values of the Nusselt number were obtained for N_{Re} up to 500. Beard and Pruppacher (1971) in a complementary work investigated the rate of evaporation of small water drops falling at terminal velocities in air. For N_{Re} larger than 2, they found that the Sherwood number was proportional to the square root of the Reynolds number, while at Reynolds number lower than 2, the Sherwood number smoothly approached the limiting value of 2 at $N_{Re} = 0$.

Pei et al. (1962, 1965) studied pure and evaporative heat transfer from spheres under combined forced and natural convection. They found that the two mechanisms of heat transfer were nonadditive and that the transition between the two was a gradual one. They also gave the

upper and lower limits of the parameter Gr/Re^2 when the effects of natural or forced convection could be neglected.

The aim of the present study was to solve the coupled momentum and energy equations for variable property flow around a sphere by numerical method. By using finite-difference approximations, the nonlinear partial differential equations are reduced to a set of nonlinear algebraic equations. Since steady state is assumed, the resulting equations are elliptic and can only be solved by iterative methods. This approach was used by Jenson (1959) and by Hamielec et al. (1967). Convergence with this method is dependent on the relaxation coefficients and on the initial guess for the flow and temperature fields.

THE NUMERICAL ANALYSIS

Description of the Model

The following assumptions were made in the mathematical formulation of the flow model:

1. The flow past the sphere is laminar and axisymmetric with zero velocity in the angular (ϕ) direction and is invariant with time.
2. The flow field is uniform and isothermal, except for the perturbations caused by the presence of the sphere.
3. The heat transferred to the sphere by convection is completely dissipated by other means, such as radiation. This balance of heat transfer results in a constant sphere temperature.
4. The physical properties of the gas are dependent on the temperature only. The heat capacity is assumed to be constant.
5. The temperature of the sphere is uniform all over the surface. Because of its relatively low level, no heat of recombination of ionized species is considered.
6. Gravity effects are not considered, and the effect of free convection on heat transfer is insignificant.
7. The fluid is extensive and an outer boundary was set for computational purposes only.
8. Viscous dissipation and compressibility effects are negligible.

The Governing Equations

The steady state continuity, Navier-Stokes, and energy equations describing the above model can be written, in spherical coordinates, as:

Stream function

$$E^2\Psi = \zeta r^3\rho \sin\theta + 1/\rho(\partial\Psi/\partial z\cdot\partial\rho/\partial z + \partial\Psi/\partial\theta\cdot\partial\rho/\partial\theta) \quad (1)$$

Vorticity

$$N_{Re}r\sin\theta/2[\partial\Psi/\partial z\cdot\partial/\partial\theta(\zeta/r\sin\theta) - \partial\Psi/\partial\theta\cdot\partial/\partial z(\zeta/r\sin\theta)] = E^2\mu\zeta r\sin\theta + \Sigma(\mu)\sin\theta - N_{Re}r\sin\theta/2\Gamma(\rho) \quad (2)$$

where

$$E^2 = \partial^2/\partial z^2 - \partial/\partial z + \sin\theta\,\partial/\partial\theta(1/\sin\theta\,\partial/\partial\theta) \quad (3)$$

$$\Sigma(\mu)/2 = \partial\mu/\partial z[\partial^2 v_r/\partial z\partial\theta + v_\theta + \partial v_r/\partial\theta + \partial^2 v_\theta/\partial\theta^2 + \partial(v_\theta\cot\theta)/\partial\theta - \partial v_\theta/\partial z] + \partial\mu/\partial\theta[v_r - \partial^2 v_r/\partial z^2 - \partial^2 v_\theta/\partial z\partial\theta - \cot\theta(\partial v_\theta/\partial z - v_\theta)] + \partial^2\mu/\partial z^2[\partial v_r/\partial\theta - v_\theta] + \partial^2\mu/\partial\theta^2[-\partial v_\theta/\partial z] + \partial^2\mu/\partial z\partial\theta[\partial v_\theta/\partial\theta + v_r - \partial v_r/\partial z] \quad (4)$$

and

$$\Gamma(\rho) = \partial\rho/\partial r(v_r\partial v_r/\partial\theta + v_\theta\partial v_\theta/\partial\theta) - \partial\rho/\partial\theta(v_r\partial v_r/\partial z + v_\theta\partial v_\theta/\partial z) \quad (5)$$

Temperature

$$(N_{Pe}r\rho/2)(v_r\partial T/\partial z + v_\theta\partial T/\partial\theta) = k[\partial^2 T/\partial z^2 + \partial T/\partial z + \partial^2 T/\partial\theta^2 + \cot\theta\,\partial T/\partial\theta] + \partial T/\partial z\cdot\partial k/\partial z + \partial T/\partial\theta\cdot\partial k/\partial\theta \quad (6)$$

The stream function modified for variable density fluid was related to the velocity components by the following equations:

$$v_r = -1/r^2\rho\sin\theta\,\partial\Psi/\partial\theta \quad (7)$$

$$v_\theta = 1/r\rho\sin\theta\,\partial\Psi/\partial r \quad (8)$$

All variables were nondimensionalized in terms of the bulk conditions of the gas; thus

$$\Psi' = \Psi/\rho_\infty U_\infty R^2 \quad \zeta' = \zeta R/U_\infty \quad r' = r/R$$
$$v_r' = v_r/U_\infty \quad v_\theta' = v_\theta/U_\infty \quad \rho' = \rho/\rho_\infty \quad \mu' = \mu/\mu_\infty$$
$$N_{Re} = 2RU_\infty\rho_\infty/\mu_\infty \quad r' = e^z \quad T' = T/T_\infty \quad k' = k/k_\infty$$
$$N_{Pe} = 2RU_\infty\rho_\infty C_p/k_\infty \quad (9)$$

The superscript on all the dimensionless variables was dropped out for simplicity. The dimensionless radial distances z allows exponential increase in r for equal increments of z. Also, when z is used, the radial spacing near the surface of the sphere is kept small while still maintaining a relatively large domain with a reasonable number of mesh points.

The thermal conductivity, viscosity, and density of argon (Amdur, 1958; Drellishak, 1963) in the temperature range of 1 500° to 5 000°K are related to the absolute temperature by the following expressions:

$$\rho = 487/T \ (\mathrm{kg\,m^{-3}})$$
$$\mu = 2\times10^{-7}T^x \ (\mathrm{kg\,s^{-1}m^{-1}})$$
$$k = 1.57\times10^{-4}T^x \ (\mathrm{Jm^{-1}s^{-1}K^{-1}}) \quad (10)$$

where $x = 0.8$ and C_p for argon is independent of the temperature, as well as the Prandtl number (0.672). In dimensionless variables

$$\rho = 1/T \quad (11)$$

$$\mu = k = T^x \quad (12)$$

Equations (11) and (12) couple the energy equation to the vorticity and the stream function equations. With the physical properties varying only with the temperature, the independent variables that characterize the flow around a sphere are the Reynolds number, Peclet number, and the dimensionless temperature.

The Boundary Conditions

The three main variables in the momentum and energy equations are the stream function, vorticity, and temperature. In the numerical solution, a few other variables were also introduced to reduce the number of calculations and the size and complexity of the difference equations. The functions F and G were defined as

$$F = \zeta/(r\sin\theta) \quad (13)$$

$$G = \mu\zeta r\sin\theta \quad (14)$$

Furthermore, when the functions Σ [Equation (4)] and Γ [Equation (5)] were evaluated, v_r and v_θ were used and not the stream function.

The boundary conditions at the sphere surface ($z = 0$) were

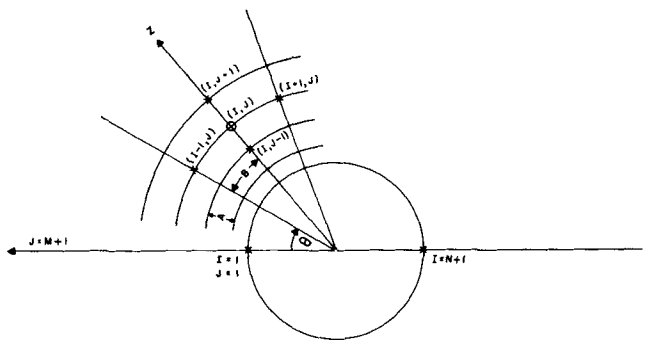

CIRCULAR MESH, Z vs. θ

Fig. 1. Circular mesh system.

$$\Psi = 0; \quad T = T_0; \quad v_r = \partial\Psi/\partial\theta = 0; \quad v_\theta = \partial\Psi/\partial z = 0$$

$$\zeta_0 = 1/\rho_0 \sin\theta \cdot \partial^2\Psi/\partial z^2 = T_0/\sin\theta \cdot \partial^2\Psi/\partial z^2$$

Also

$$F = \zeta_0/\sin\theta$$

$$G = \mu_0\zeta_0 \sin\theta = T_0{}^x\zeta_0 \sin\theta$$

The conditions at the outer boundary ($z = z_\infty$) were

$$\Psi = r_\infty{}^2 \sin^2\theta/2; \quad \zeta = F = G = 0; \quad T = 1;$$

$$v_r = -\cos\theta; \quad v_\theta = \sin\theta$$

The conditions along the axis of symmetry were

At $\theta = 0$ deg:

$$\Psi = 0; \quad \zeta = G = 0; \quad \partial T/\partial\theta = 0; \quad v_\theta = 0;$$

$$v_r = -1/(\rho_r{}^2 \sin\theta) \cdot \partial\Psi/\partial\theta; \quad F = \zeta/r \sin\theta$$

Since $\sin\theta = 0$ at $\theta = 0$ deg, v_r and F had to be found by taking the limits as θ approached zero; thus

$$v_r = (-1/\rho r^2)(\partial^2\Psi/\partial\theta^2); \quad F = (1/r)(\partial\zeta/\partial\theta)$$

At $0 = 180$ deg:

$$\Psi = 0; \quad \zeta = G = 0; \quad \partial T/\partial\theta = 0; \quad v_\theta = 0;$$

$$v_r = (1/\rho r^2)(\partial^2\Psi/\partial\theta^2); \quad F = -(1/r)(\partial\zeta/\partial\theta)$$

The Difference Equations

The stream function, vorticity, and temperature equations were transformed from their original partial differential form to a set of algebraic equations by first dividing the flow field into a large number of mesh points and then approximating the variables at each point by Taylor series. The derivatives were determined in terms of adjacent points, using the central difference method accurate up to the order of (h^2). Figure 1 illustrates the circular mesh used. The governing equations thus become:

Stream function

$$[\Psi(I,J+1)(2-A) + \Psi(I,J-1)(2+A)]/2A^2 + [\Psi(I+1,J)(2-B\cot\theta) + \Psi(I-1,J)(2+B\cot\theta)]/2B^2 - \Psi(I,J)(2/A^2 + 2/B^2) - \zeta(I,J)r^3 \sin\theta/T(I,J) + 1/T(I,J)[\partial\Psi/\partial z \cdot \partial T/\partial z + \partial\Psi/\partial\theta \cdot \partial T/\partial\theta] = 0 \quad (15)$$

Vorticity

$$[G(I,J+1)(2-A) + G(I,J-1)(2+A)]/2A^2 + [G(I+1,J)(2-B\cot\theta) + G(I-1,J)(2+B\cot\theta)]/2B^2 - G(I,J)(2/A^2 + 2/B^2) + \Sigma(\mu)\sin\theta - Re\, r \sin\theta/2\Gamma(\rho) + Re\, r \sin\theta/4\{\partial\Psi/\partial\theta[F(I,J+1) - F(I,J-1)]/A - \partial\Psi/\partial z[F(I+1,J) - F(I-1,J)]/B\} = 0 \quad (16)$$

where

$$\Sigma(I,J) = 2xT(I,J)^{x-1}\{\partial T/\partial\theta[v_r(I,J) - \partial^2 v_r/\partial z^2 - \partial^2 v_\theta/\partial z\partial\theta - \cot\theta(\partial v_\theta/\partial z - v_\theta(I,J))] + \partial T/\partial z[\partial v_r/\partial z\partial\theta + \partial v_r/\partial\theta + \partial^2 v_\theta/\partial\theta^2 - \partial v_\theta/\partial z + \cot\theta(\partial v_\theta/\partial\theta - \cot\theta\, v_\theta(I,J))] + (x-1)/T(I,J)[\partial^2 T/\partial z^2(\partial v_r/\partial\theta - v_\theta(I,J)) - \partial^2 T/\partial\theta^2 \cdot \partial_\theta{}^v/\partial z + \partial^2 T/\partial z\partial\theta(\partial v_\theta/\partial\theta + v_r(I,J) - \partial v_r/\partial z)]\} \quad (17)$$

$$\Gamma(I,J) = -1/T(I,J)^2\{\partial T/\partial z[v_r(I,J)\cdot\partial v_r/\partial\theta + v_\theta(I,J)\partial v_\theta/\partial\theta] - \partial T/\partial\theta[v_r(I,J)\partial v_r/\partial z + v_\theta(I,J)\partial v_\theta/\partial z]\} \quad (18)$$

and the velocity components are defined as

$$v_r(I,J) = -T(I,J)[\Psi(I+1,J) - \Psi(I-1,J)]/(2Br^2 \sin\theta) \quad (19)$$

$$v_\theta(I,J) = T(I,J)[\Psi(I,J+1) - \Psi(I,J-1)]/(2Ar^2 \sin\theta) \quad (20)$$

Energy

$$[T(I,J+1)(2+A) + T(I,J-1)(2-A)]/2A^2 + [T(I+1,J)(2+B\cot\theta) + T(I-1,J)(2-B\cot\theta)]/2B^2 - T(I,J)(2/A^2 + 2/B^2) + Pe/[2r\sin\theta\, T(I,J)^x](\partial\Psi/\partial\theta \cdot \partial T/\partial z - \partial\Psi/\partial z \cdot \partial T/\partial\theta) + x/T(I,J)[(\partial T/\partial z)^2 + (\partial T/\partial\theta)^2] = 0 \quad (21)$$

For simplicity, some of the derivatives in the difference equations are written in their differential form. The difference equivalent of these derivatives can be obtained by direct substitution into the finite-difference equations.

Boundary conditions

At $z = 0$:

$$\Psi(I,1) = 0; \quad v_\theta(I,1) = 0; \quad v_r(I,1) = 0;$$

$$T(I,1) = T_0; \quad \zeta(I,1) = T_0 \cdot [8\Psi(I,2) - \Psi(I,3)]/2A^2 \sin\theta$$

$$G(I,J) = T_0{}^x\zeta(I,1)\sin\theta; \quad F(I,1) = \zeta(I,1)/\sin\theta$$

At $z = z_\infty$:

$$\Psi(I,M+1) = r_\infty \sin^2\theta/2; \quad \zeta(I,M+1) = 0;$$

$$F(I,M+1) = G(I,M+1) = 0; \quad T(I,M+1) = 1;$$

$$v_\theta(I,M+1) = \sin\theta; \quad v_r(I,M+1) = -\cos\theta$$

At $\theta = 0$:

$$\Psi(1,J) = 0; \quad \zeta(1,J) = 0;$$

$$T(1,J) = [4T(2,J) - T(3,J)]/3; \quad v_\theta(1,J) = 0;$$

$$v_r(1, J) = -2T(1, J)\Psi(2, J)/B^2r^2;$$

$$F(1, J) = \zeta(2, J)/Br; \quad G(1, J) = 0$$

At $\theta = \pi$:

$$\Psi(N + 1, J) = 0; \quad \zeta(N + 1, J) = 0;$$

$$T(N + 1, J) = [4T(N, J) - T(N - 1, J)]/3;$$

$$v_\theta(N + 1, J) = 0; \quad v_r(N + 1, J) = 2T(N + 1, J)$$

$$\Psi(N, J)/B^2r^2; \quad F(N + 1, J) = -\zeta(N, J)/Br;$$

$$G(N + 1, J) = 0$$

The above algebraic equations cannot be solved directly because of their nonlinearity. Hence, an iterative procedure was used. The most appropriate iteration method is the successive over relaxation (SOR) method, where a relaxation factor is used to control the speed of convergence of the process and to maintain its stability.

The Relaxation Procedure

Equations (15), (16), and (21) can be written in a general form as

$$\Phi(I, J) = f[\Phi(I + 1, J), \Phi(I - 1, J), \Phi(I, J + 1), \Phi(I, J - 1)] \quad (22)$$

The new value of function $\Phi(I, J)$ is calculated using the latest values of the variables in the adjacent points. Replacing this new value directly into the grid can cause instabilities which may lead to divergence. To avoid this, the new value of the function that is placed in the grid is chosen somewhere between the old and the calculated value; thus

$$\Phi_{new} = \Phi_{old} + W(\Phi_{calc} - \Phi_{old}) \quad (23)$$

W is known as the relaxation coefficient. The optimum value of the relaxation coefficient that will give the fastest convergence depends on the mesh, the shape of the domain, the type of boundary conditions, and on the nature of the equations (Roache, 1972). Roache (1972) and Lapidus (1962) gave methods for calculating the optimum relaxation coefficients for linear elliptic equations. No such methods are available when the equations are nonlinear. Moreover, because of the large computation times required for solving a set of nonlinear equations, it is not practical to conduct a systematic study of the effect of different relaxation coefficients on the rate of convergence. In such instances, the relaxation coefficients are chosen by trial and error, and their value is specific to the system under consideration. Usually, the selection of the relaxation coefficient is based on the highest value that does not cause instabilities.

For nonlinear problems, there is no reason for assuming that the optimum relaxation coefficient has the same value over the entire flow field. In the logarithmic grid of the present study, the mesh size increased exponentially with radial distance away from the surface resulting in an increased instability near the outer boundary. Therefore, small values of the relaxation coefficient near the outer boundary were necessary to reduce error propagation and to dampen oscillations.

The general form of a second-order elliptic equation is

$$\nabla^2_{xy}\Phi = P\partial\Phi/\partial x + Q\partial\Phi/\partial y \quad (24)$$

Woo (1970) derived the following expression for the relaxation coefficients to be used in the solution of the above equation

$$W_{\Phi i,j} = 2/[1 + \sqrt{0.5(P^2 + Q^2)}] \quad (25)$$

and for the linear Poisson's equation:

$$W_\Psi = 2/[1 + \pi\sqrt{0.5(N^{-2} + M^{-2})}] \quad (26)$$

Woo found that for linear equations, such as constant property heat transfer to a sphere, convergence with these relaxation coefficients was much faster than when constant factors were used. No such comparison was possible for the nonlinear problem, where the relaxation coefficients had to be evaluated at every step, since P and Q were continuously changed during the computation. Fortunately, Woo found that these coefficients (P and Q) did not vary much from one iteration to the other and, thus, had to be recalculated only once in every K iterations. K was of the order of 20.

The values of P and Q were found from Equations (2) and (6):

$$P_\zeta = N_{Re}/2r \sin\theta\, \partial\Psi/\partial z \quad (27)$$

$$Q_\zeta = -N_{Re}/2r \sin\theta\, \partial\Psi/\partial\theta \quad (28)$$

$$P_T = N_{Pe}/2r \sin\theta\, \partial\Psi/\partial z \quad (29)$$

$$Q_T = -N_{Pe}/2r \sin\theta\, \partial\Psi/\partial\theta \quad (30)$$

A computer program was written for the simultaneous solution of the governing equations by the above iteration method. Direct substitution ($W = 1$) and varying relaxation coefficients were applied alternately on the mesh points to calculate the new values of the vorticity, stream function, and temperature. The independent variables of the program were the Reynolds number, Peclet number, dimensionless surface temperature, and the property exponent x. The program, however, did not give the constant property solution when x was set to zero because the variation of the density with temperature was still included in the equations. This less general set of equations was found to require less computations, as compared to that where the properties were evaluated individually at every point. To obtain the constant property solution, a separate program was written. Since the simpler constant property equations were used in this program, the energy equation was no longer coupled to the momentum equations, and thus the former was solved after the flow field had been calculated.

Computation Sequence

The number of iterations required to reach convergence depends on the nature of the problem, the relaxation coefficients used, and on the initial guess. Starting with a guess that was far from the condition under study caused instabilities and required the use of very low relaxation coefficients which in turn led to an increase in the number of iterations. To overcome this problem, the solutions were obtained in small faster steps, through which the Reynolds number and the surface temperature T_0 were changed gradually.

The complexity of the equations under study prevented a systematic investigation of the exact effects of lattice spacing and field size on the accuracy of the solutions, in order to permit the selection of an optimum mesh. Woo (1970) studied the constant property problem extensively and made some recommendations on the optimum mesh and field sizes. These guidelines were used in this study, where two different mesh sizes were used for the low and the intermediate Reynolds number ranges; thus

N_{Re}	Δz	M	r_∞	$\Delta\theta$	N
0.1 – 1	0.1	40	54.6	6 deg	30
10 – 50	0.05	40	7.39	6 deg	30

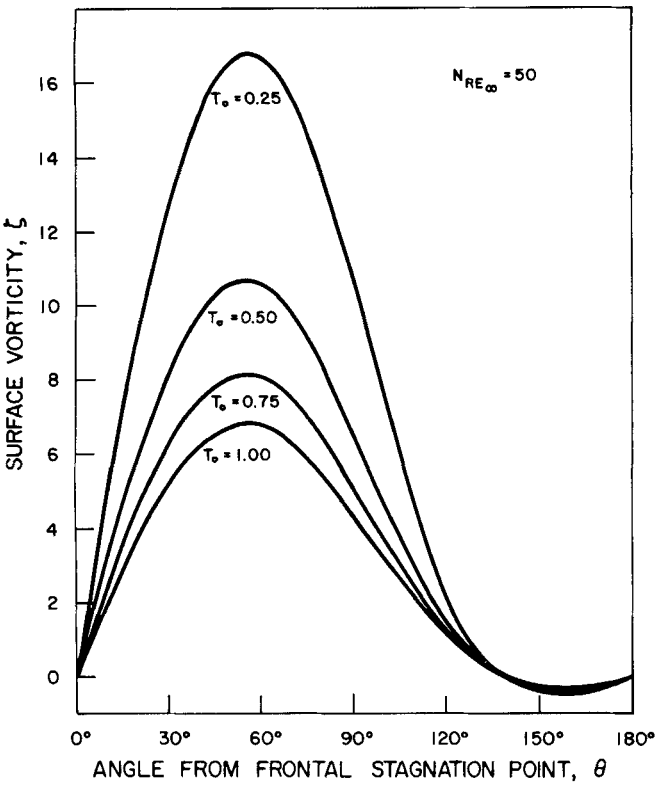

Fig. 2. Effect of surface temperature on surface vorticity distribution $N_{Re_\infty} = 50$.

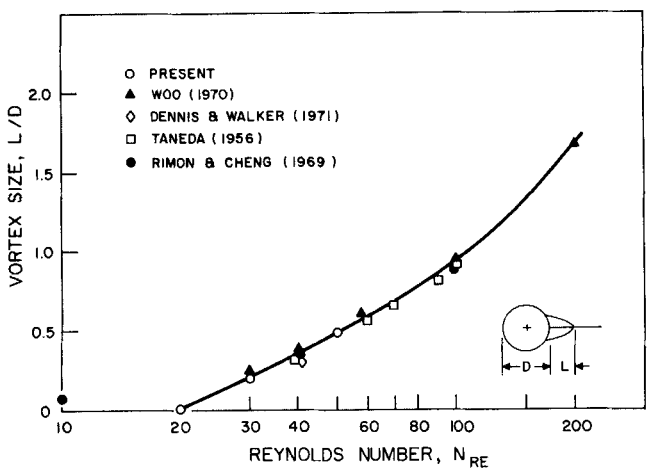

Fig. 4. Effect of Reynolds number on vortex length L/D for constant property flow.

The convergence criterion in this study was based on maximum absolute error in the temperature and vorticity. When the change in these variables between successive iterations was less than the tolerance, at every lattice point the computation process was stopped and the Nusselt number and the drag coefficients calculated. These were also calculated once every K iterations. The tolerance was 10^{-5} for low N_{Re} and went up to 10^{-3} at Reynolds number of 50. As the computation times became excessive, the calculations were stopped when the variations in the Nusselt number and the drag coefficients from one iteration to the other were small. It was felt that very accurate solutions were not quite necessary

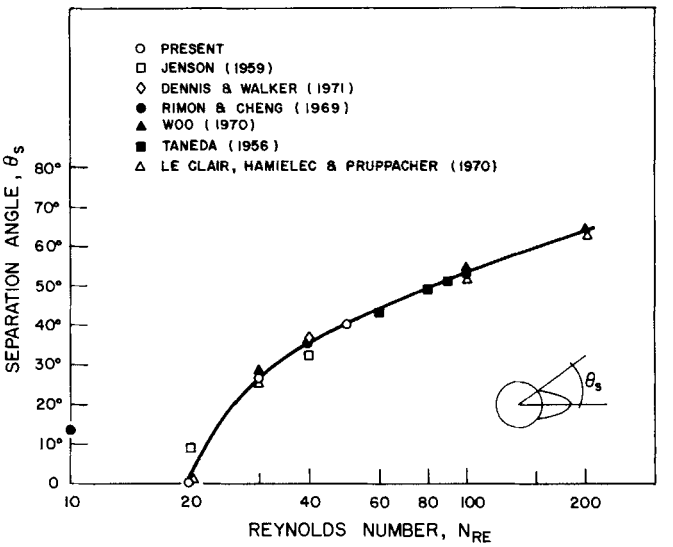

Fig. 3. Effect of Reynolds number on separation angle Θ_s for constant property flow.

TABLE 1

N_{Re}	$T_0 = 1.0$	$T_0 = 0.75$	$T_0 = 0.50$	$T_0 = 0.25$
		Separation angle, Θ_s		
20	—	11.0 deg	13.5 deg	12.5 deg
30	26.5 deg	28.5 deg	30.5 deg	28.5 deg
50	40.0 deg	41.0 deg	42.0 deg	42.5 deg
		Vortex length, L/D		
20	—	0.02	0.03	0.03
30	0.22	0.20	0.21	0.22
50	0.48	0.54	0.55	0.52

since, in practice, the flow variables in high temperature environments are not known to such an accuracy as to justify the increase in the computation work.

RESULTS AND DISCUSSION*

Flow Field

The surface vorticity distributions for $N_{Re_\infty} = 50$ and $0.25 \leq T_0 \leq 1.0$ are shown in Figure 2. T_0 is the ratio of the temperature of the sphere surface to that of the gas stream. The effect of the Reynolds number and T_0 on the angle of separation θ_s and on the vortex length expressed as the ratio L/D are listed in Table 1. For the correct interpretation of the data which will be presented in the rest of this paper, it should be remembered that $T_0 = 1$ denotes isothermal and therefore constant property conditions. For $T_0 < 1$, the surface temperature of the sphere is lowered with respect to that of the gas stream.

It can be observed from Figure 2 and Table 1 that outside of the large effect on the surface vorticity, the decrease in the sphere surface temperature had little effect on the overall trends of the flow. At a specific Reynolds number, the maximum value of the surface vorticity occurred at the same angle at all T_0 values. Flow separation point and vortex size were also only marginally affected by the decrease in the surface temperature.

The actual vorticity values, however, became very much higher as T_0 decreased, actually increasing exponentially

* The complete results of the numerical analysis can be found in the thesis by N. N. Sayegh (1977).

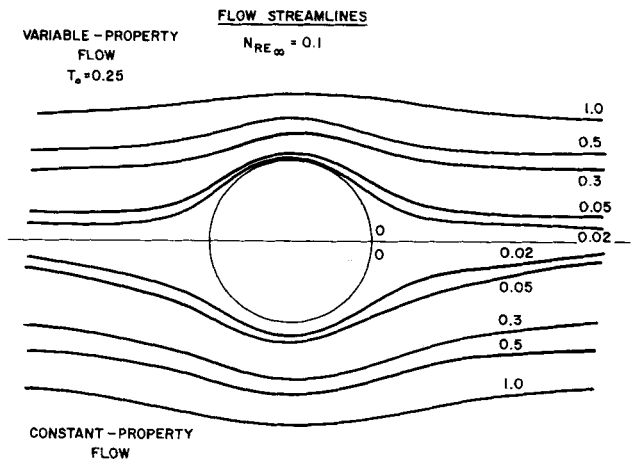

Fig. 5. Streamlines for constant and variable property flows at $T_0 = 0.25$ $N_{Re_\infty} = 0.1$.

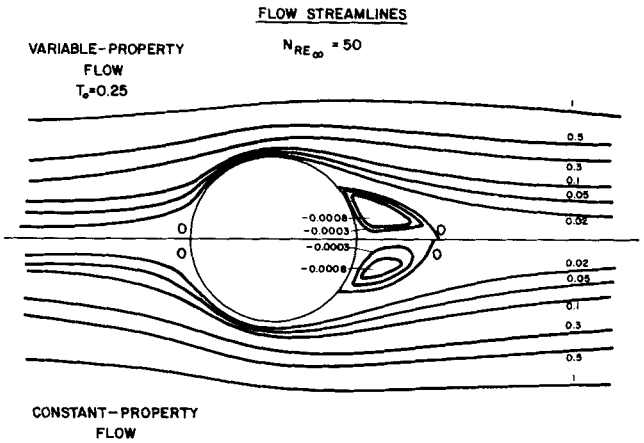

Fig. 6. Streamlines for constant and variable property flows at $T_0 = 0.25$ $N_{Re_\infty} = 50$.

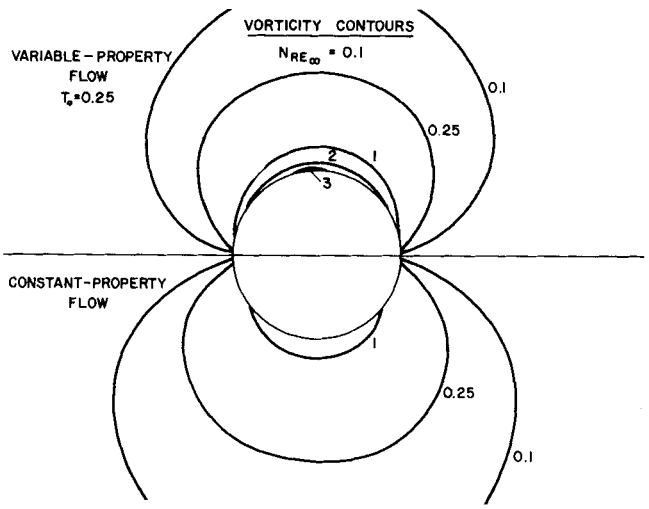

Fig. 7. Vorticity contours for constant and variable property flows at $T_0 = 0.25$ $N_{Re_\infty} = 0.1$.

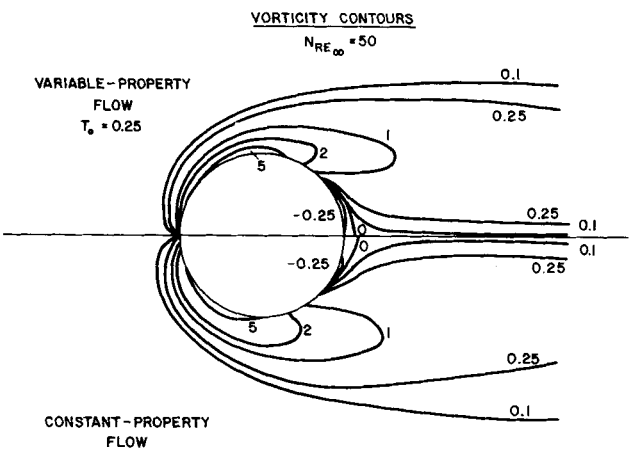

Fig. 8. Vorticity contours for constant and variable property flows at $T_0 = 0.25$ $N_{Re_\infty} = 50$.

with a decrease in T_0. This is attributed to higher velocities and hence steeper velocity gradients near the surface caused by a decrease in the fluid viscosity. It is certainly the most striking feature of the vorticity calculations.

Figures 3 and 4 compare the separation angle and vortex lengths obtained in this study for constant property flow ($T_0 = 1$) with experimental and theoretical results reported in the literature. Very good agreement is indicated, thus demonstrating the validity of the model and of the numerical analysis. It was not possible to present a similar comparison for the variable property case owing to the unavailability of pertinent data.

Figures 5 to 8 show the streamlines and vorticity contours for constant property flow and the variable property

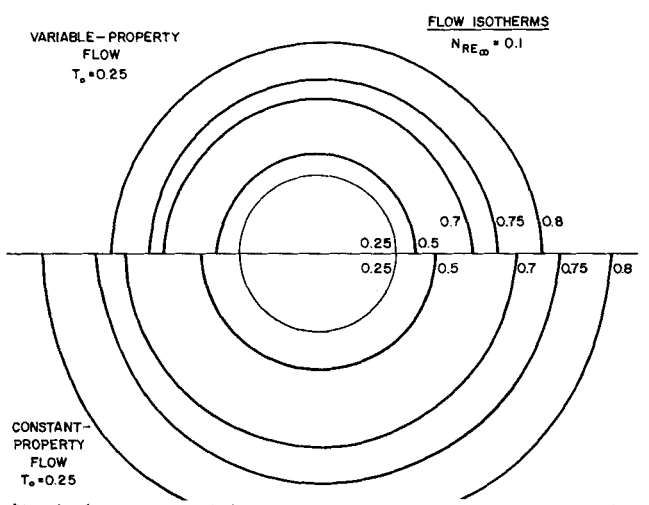

Fig. 9. Temperature fields for constant and variable property flows at $T_0 = 0.25$ $N_{Re_\infty} = 0.1$.

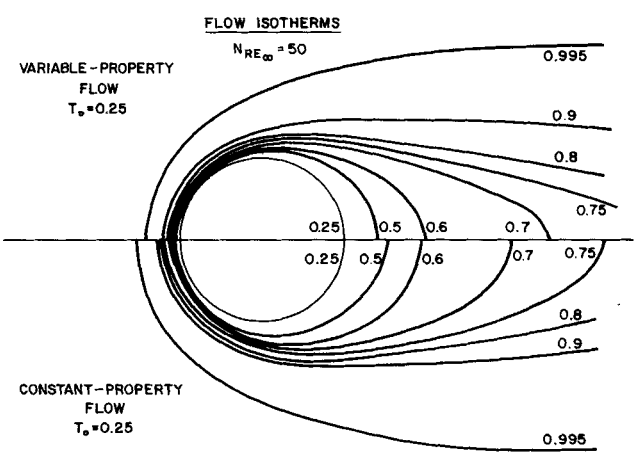

Fig. 10. Temperature fields for constant and variable property flows at $T_0 = 0.25$ $N_{Re_\infty} = 50$.

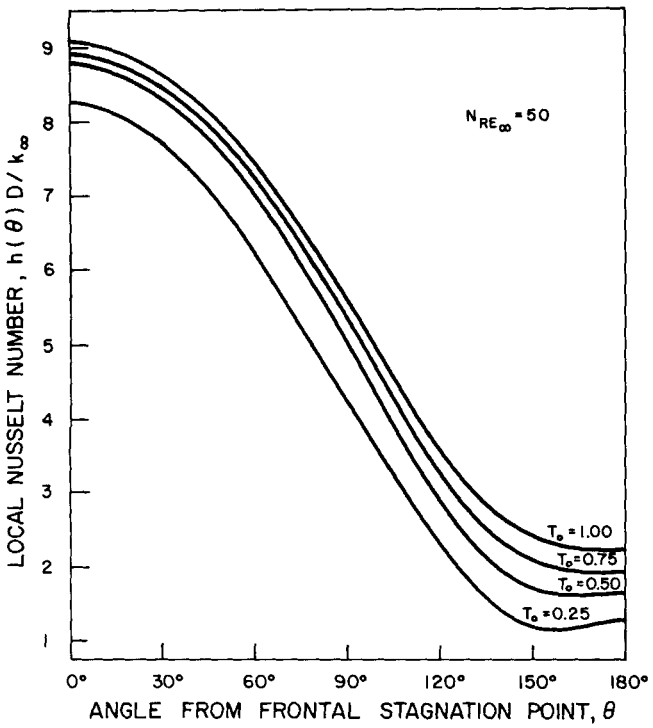

Fig. 11. Effect of surface temperature on local Nusselt number distribution $N_{Re_\infty} = 50$.

case at $T_0 = 0.25$ for $N_{Re} = 0.1$ and 50. Here again, the general shape of the flow field did not change significantly with departure from isothermal conditions. The streamlines, however, moved closer as the surface temperature was reduced. This was partly caused by an increase in the fluid density accompanied with little change in the

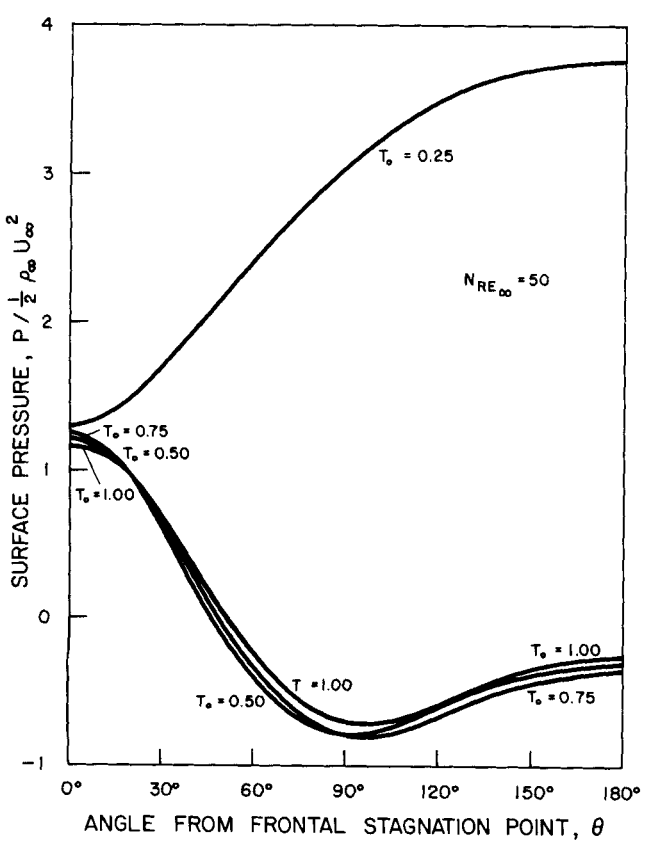

Fig. 13. Effect of surface temperature on surface pressure distribution $N_{Re_\infty} = 50$.

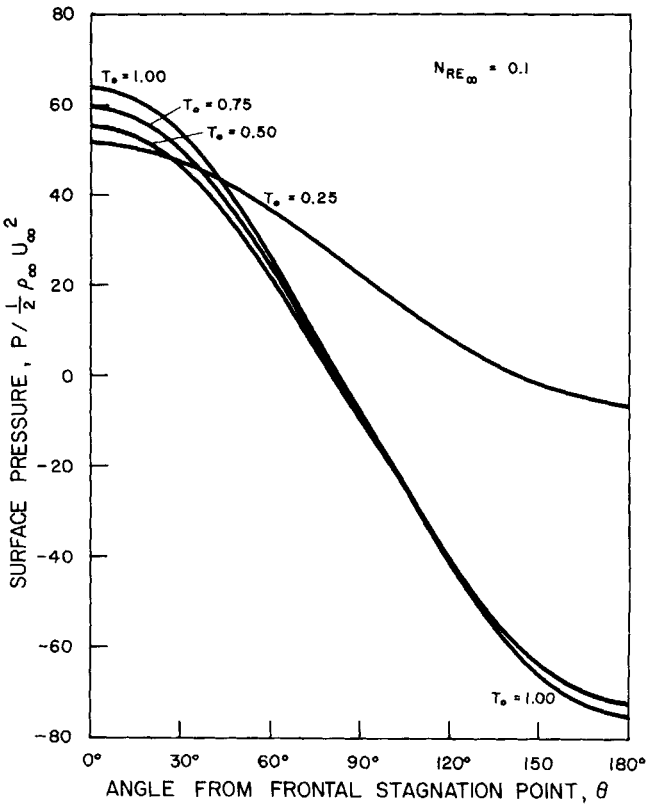

Fig. 12. Effect of surface temperature on surface pressure distribution $N_{Re_\infty} = 0.1$.

velocity and partly due to lower viscosity which was the main reason for higher velocities near the surface. For the same reasons, the recirculation in the wake was much faster for colder sphere surfaces, while the actual size of the vortex was approximately the same as for the constant property case. The presence of low viscosity, higher density, and velocity near the surface, as that experienced in the variable property case, should effect a much earlier separation. This, however, was not the case owing to the complex interaction between the steep velocity, temperature, and property gradients near the surface. A detailed discussion of these phenomena is beyond the scope of this paper.

Temperature Field and Local Nusselt Numbers

The temperature fields for constant property flows and variable property flows at $T_0 = 0.25$ are shown in Figures 9 and 10 for $N_{Re} = 0.1$ and 50. Figure 11 is a plot of

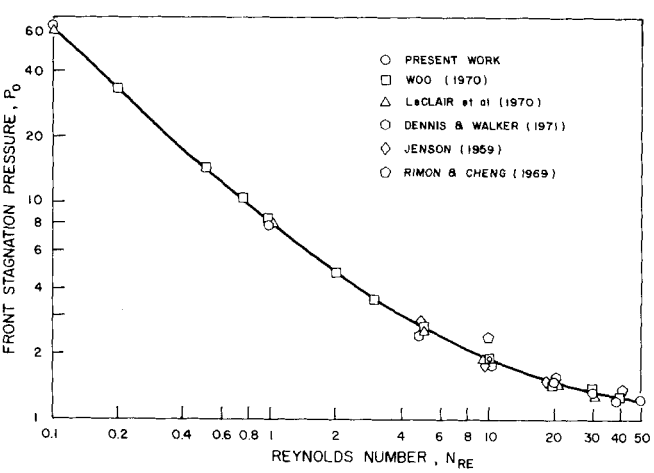

Fig. 14. Variation of front stagnation pressure with the Reynolds number for constant property flow.

TABLE 2

N_{Re}	$T_0 = 1.0$	$T_0 = 0.75$	$T_0 = 0.50$	$T_0 = 0.25$
		Friction drag coefficients		
0.1	168.4	148.1	129.2	103.8
1	18.45	16.56	14.63	12.42
10	2.96	2.69	2.46	2.19
20	1.07	1.65	1.52	1.37
30	1.35	1.26	1.16	1.04
50	0.96	0.90	0.84	0.77
		Pressure drag coefficient		
0.1	82.3	87.7	85.0	38.0
1	9.04	9.90	9.70	2.90
10	1.63	1.77	1.89	0.33
20	1.79	1.18	1.21	−0.61
30	0.86	0.95	0.93	−1.04
50	0.67	0.72	0.66	−1.52
		Total drag coefficient		
0.1	250.6	235.8	214.1	146.2
1	27.49	26.46	24.33	15.32
10	4.59	4.46	4.36	2.52
20	2.86	2.83	2.73	0.76
30	2.21	2.21	2.10	0.007
50	1.62	1.62	1.50	−.075

the local Nusselt number distributions along the sphere surface for $N_{Re\infty} = 50$ and $0.25 \leq T_0 \leq 1$. All of the Nusselt numbers were evaluated at free stream conditions (same k_∞) to allow comparison between different surface temperature conditions.

Once again, the change in the surface temperature affected the level of the temperature only and not the general pattern of the temperature field. The variable property flow isotherms moved closer to each other as the surface temperature was decreased, resulting in higher temperature gradients at the surface than in the constant property case. This increase in the temperature gradient, however, did not result in higher heat transfer rates or Nusselt numbers (see Figure 11), since the decrease of the surface temperature was accompanied by a similar reduction in the thermal conductivity of the gas near the surface.

Surface Pressure Distribution

Figures 12 and 13 show the surface pressure distributions for $N_{Re} = 0.1$ and 50. It can be observed that at low Reynolds numbers ($N_{Re} = 0.1$) the effect of decreasing the surface temperature was a lowering in the value of the front stagnation pressure p_0. On the other hand, for intermediate values of the Reynolds number, this influence was reversed, and p_0 attained higher values at lower surface temperatures. The stagnation pressure equation can be written in the following simplified form:

$$p_0 = \text{inertia term} + 8/N_{Re}\ [\text{viscous term}]$$

As the surface temperature is lowered, the density of the fluid increases, resulting in higher inertia forces. On the other hand, lower surface temperature reduces viscous forces by reducing fluid viscosity near the sphere. At low Reynolds number, the viscous forces are predominating, and by reducing them, the front stagnation pressure is also reduced. However, at higher Reynolds numbers, the inertia forces gain importance, leading to higher p_0 values at lower temperatures.

Figures 12 and 13 show that for the studied range of the Reynolds numbers and $T_0 \geq 0.5$, the effect of varying

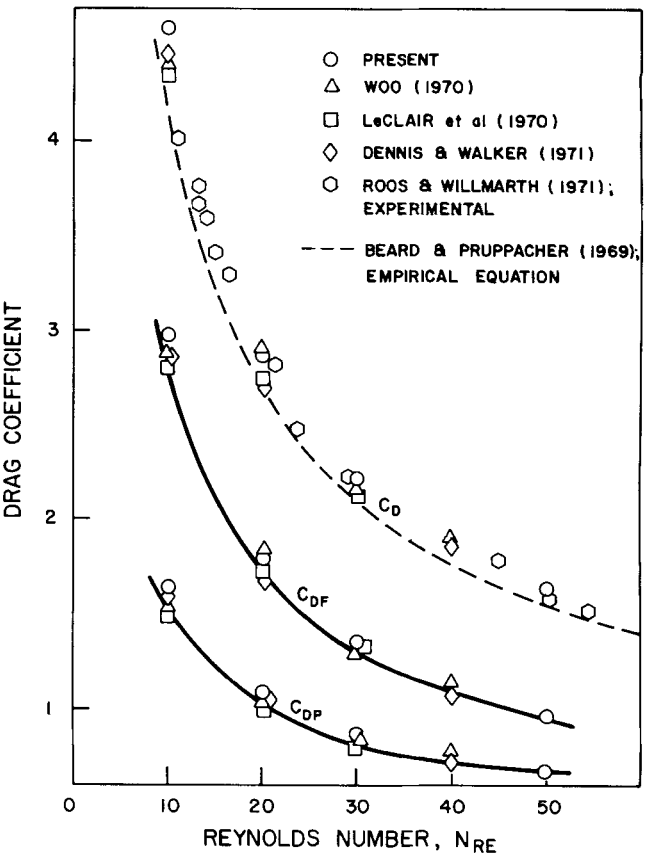

Fig. 15. Variation of friction, pressure and total drag coefficients with the Reynolds number for constant property flow.

TABLE 3. OVERALL NUSSELT NUMBER hD/k_∞

N_{Re} UD/ν_∞	$T_0 = 1.0$*	$T_0 = 0.75$	$T_0 = 0.50$	$T_0 = 0.25$
0.1	2.021	1.918	1.687	1.370
1	2.232	2.123	1.879	1.526
10	3.323	3.161	2.924	2.537
20	4.022	3.872	3.614	3.136
30	4.560	4.425	4.143	3.584
50	5.411	5.281	4.979	4.313

* $T_0 = 1.0$ refers to constant property solution.

fluid properties on the surface pressure distribution was not very marked. However, at $T_0 = 0.25$, the surface pressure gradient $\partial p/\partial\theta$ became less steep, and at $N_{Re} > 20$ its direction changed from negative to positive. Consequently, the surface pressure increased with θ leading to $p(\pi) > p_0$. It is important to note that the trend first exhibited in Figure 12 went right through all the Reynolds numbers studied. There was no discontinuity in the behavior which might indicate a faulty numerical technique. The explanation for this phenomenon can be deduced from the Navier-Stokes equation. At the sphere surface, the inertia forces are equal to zero because of the no-slip condition. Hence, the change in the momentum transfer by viscous forces is balanced by an equal change in the pressure force. The rate of momentum gain by viscous transfer in the θ direction at the sphere surface is proportional to $\partial(-\mu\zeta r)/dz$. For constant property flow, the viscosity is constant, and the change in momentum is positive since $\partial\zeta r/\partial z$ is negative. Consequently, the change in the pressure force is negative. However, when the viscosity is also changing with radial position,

the overall change in momentum transfer can be either negative or positive, depending on the relative magnitude of the viscosity and velocity gradients.

From a purely physical point of view, it must be admitted that the behavior at $T_0 = 0.25$ is highly anomalous. The increase in surface pressure at $N_{Re} > 20$ predicted by the numerical analysis is extremely difficult to reconcile with the classical physical visualization of boundary-layer flow. Flow without separation in the presence of such large positive pressure gradients could only be sustained if the boundary layer were turbulent, the transition occurring in the frontal region of the sphere. A turbulent boundary layer would also account for the very low total drag coefficients, reported in the next section, under these conditions. It must be emphasized, however, that the numerical analysis was entirely based on laminar flow considerations. The solutions would, therefore, be invalid if turbulence were present. Nor can the analysis predict the onset of turbulence. The interpretation must, therefore, be strictly based on the momentum transfer considerations mentioned above.

In Figure 14, the values of the front stagnation pressure for constant property flow were plotted vs. the Reynolds number. A very good agreement between the present results and the results of others can be observed.

Drag Coefficients

The values of the friction, pressure and total drag coefficients are listed in Table 2. Since the friction drag is directly proportional to the viscosity and inversely proportional to the Reynolds number, it decreased monotonically with increasing N_{Re} and decreasing T_0. The pressure drag is a result of differences in the pressure over the sphere surface and is, therefore, directly related to the shape of the pressure distribution curve. As was discussed earlier, for $T_0 \geq 0.5$, the effect of decreasing

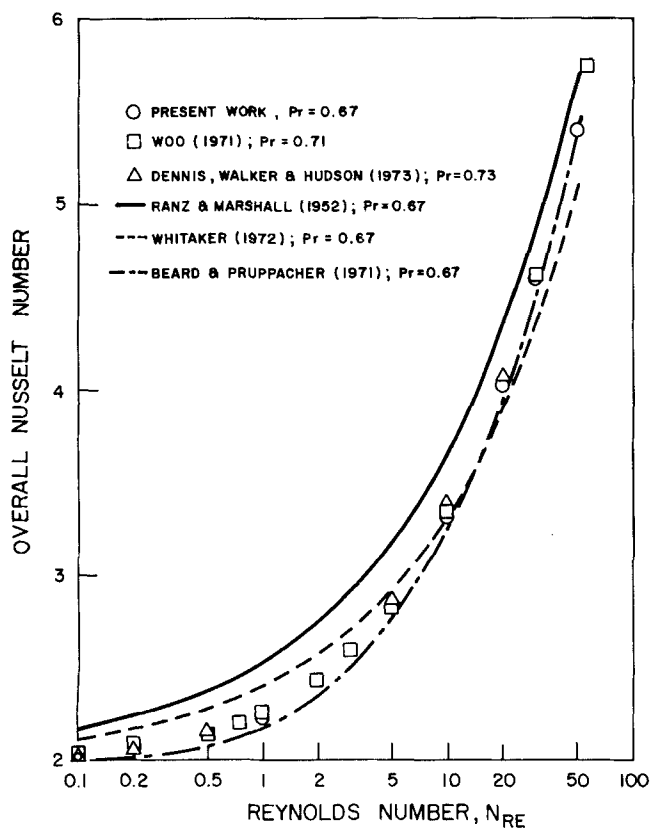

Fig. 16. Variation of the overall Nusselt number with the Reynolds number for constant property flow.

T_0 on $p(\theta)$ was small, and consequently the variation of C_{DP} with T_0 is also small. At $T_0 = 0.25$, however, the shape of $p(\theta)$ vs. θ curves was drastically changed, and hence the pressure drag coefficients were significantly reduced.

The constant property drag coefficients obtained in this study are compared in Figure 15 with experimental and theoretical results of other works. The present results are slightly higher than most of the rest. This discrepancy is possibly due to the closer outer boundaries selected for the present analysis ($r_\infty = 7.4$) as compared to $r_\infty = 90$ in LeClair's (1970) solution.

Correlation of Heat Transfer Results

The values of the overall Nusselt number for all of the cases studied are listed in Table 3. In the following analysis, a correlation will be derived for constant property flow which will then be modified to include the effect of variable properties.

Constant Property Transfer. In Figure 16, the constant property results of this study are compared with the theoretical results of Woo (1970) and Dennis et al. (1973) and to the experimental equations of Whitaker (1972), Beard and Pruppacher (1971), and Ranz and Marshall (1952). Excellent agreement can be observed among the theoretical results, including those of the present study. The experimental correlations, however, are accurate for only very small ranges of the Reynolds number. A new correlation will, therefore, be proposed here to fit the numerical results. The general form of the equation will be assumed to be

$$N_{Nu} = a + bN_{Pr}{}^{m}N_{Re}{}^{n} \tag{31}$$

a is the limiting Nusselt number at $N_{Re} = 0$. For a sphere immersed in a constant property fluid, a has the value of 2. The exponents m and n need not necessarily be constants.

In the present work, only one value of the Prandtl number was studied, namely, $N_{Pr} = 0.67$. Consequently, it was not possible to investigate the effect of the Prandtl number from the results.

Woo (1970) solved the energy equation for N_{Re} between 1 and 300 and $0.25 < N_{Pr} < 5$. Based on Equation (31), the exponent m in the range $0.5 < N_{Pr} < 2$ can be derived from Woo's results as

$$m = 0.78\, N_{Re}{}^{-0.145} \tag{32}$$

for $0.2 < N_{Re} < 100$. For $N_{Re} < 0.2$, m approaches the value of unity and at high N_{Re} (>100) a value of 0.435. Using Equation (32), the Nusselt number dependence on Re and Pr was found to be

$$Nu = 2 + 0.473\, N_{Pr}{}^{m}N_{Re}{}^{0.552} \tag{33}$$

Variable Property Transfer. For the limiting case of the Reynolds number approaching zero, the Nusselt number for a sphere submerged in an infinite constant property fluid approaches a value of 2, which represents conduction heat transfer. This value, however, deviates from 2 for variable property fluids owing to the variation of the gas conductivity with radial distance away from the sphere. The energy equation at zero N_{Re} reduces to

$$(1/r^2)d(r^2q_r)/dr = 0 \tag{34}$$

Substituting the relation between k and T into the above equation and integrating between the limits of the sphere surface and infinity, we get in dimensionless variables (that is, $T' = T/T_\infty$; $r' = r/r_\infty$)

$$T'^{(1+x)} = 1 - (1/r')(1 - T_0{}^{1+x}) \tag{35}$$

The overall Nusselt number based on properties evaluated at the surface temperature, in dimensionless variables, is given by

$$N_{Nu0} = 1/(1 - T_0) \int_0^{\pi} dT'/dr'|_{r'=1} \sin\theta \, d\theta \quad (36)$$

Substituting Equation (35) and integrating, we get, for $N_{Re} = 0$

$$N_{Nu0} = hD/k_s = 2(1 - T_0^{1+x})/[(1 + x)(1 - T_0)T_0^x] \quad (37)$$

When we use a dimensionless reference temperature T_f instead of T_0 to evaluate the thermal conductivity, the above equation becomes

$$N_{Nuf} = hD/k_f = 2(1 - T_0^{1+x})/[(1 + x)(1 - T_0)T_f^x] \quad (38)$$

Equation (31) for constant property transfer can now be modified to include the effect of variable properties; thus

$$N_{Nufk} = 2 f_{fk} + 0.473 N_{Pr}^m N_{Ref\nu}^{0.552} \quad (39)$$

where

$$f_{fk} = (1 - T_0^{1+x})/[(1 + x)(1 - T_0)T_{fk}^x] \quad (40)$$

In this equation, the Nusselt number is evaluated at reference temperature T_{fk} and the Reynolds number at $T_{f\nu}$. Reference temperatures are used to account for changing physical properties in the flow field. Since the thermal conductivity and the kinematic viscosity do not change in the flow field in exactly the same manner, nor is their effect on the heat transfer process identical, there is no justification for presuming that the reference temperatures at which N_{Re} and N_{Nu} are evaluated are the same. Obviously, the function f should be evaluated at the same temperature as N_{Nu}.

From the numerical results it was found that Equation (39) gave the best fit when the Nusselt number was evaluated at surface temperature and the Reynolds number at $T_{0.19}$, defined as

$$T_{0.19} = T_s + 0.19(T_\infty - T_s) \quad (41)$$

The exponent of the Prandtl number in Equation (32) was calculated using $N_{Re0.19}$.

A common practice in the past for accounting for variable property variations has been to multiply the heat transfer equation by a property ratio raised to a certain power. This method was not used in the present analysis for two reasons: the equation does not reduce to the variable property limiting Nusselt number at $N_{Re} = 0$ and there is no theoretical justification for this property ratio.

Summarizing, the heat transfer correlation derived from the numerical analysis is

$$N_{Nu0} = 2 f_0 + 0.473 N_{Pr}^m N_{Re0.19}^{0.552} \quad (42)$$

where

$$m = 0.78 N_{Re0.19}^{-0.145} \quad (43)$$

$$2f_0 = 2(1 - T_0^{1+x})/[(1 + x)(1 - T_0)T_0^x] = \text{limiting } N_{Nu} \quad (44)$$

$$N_{Re0.19} = UD/\nu_{0.19} \quad (45)$$

This equation reduces to Equation (33) for constant property heat transfer.

In closing, it should be noted that since the present study was completed, the authors have had an opportunity of carrying out an experimental investigation of the rate of heat transfer to spheres exposed to an argon plasma jet. The experimental results, which will be published soon, are in good agreement with the theoretical predictions of the present paper.

ACKNOWLEDGMENT

The authors wish to express their appreciation for the financial support provided by the National Research Council of Canada and by the Ministry of Education of the Province of Quebec.

NOTATION

A = lattice spacing in z direction
a = constant, Equation (31)
B = lattice spacing in θ direction
b = constant, Equation (31)
c_p = heat capacity at constant pressure
D = diameter of sphere
E^2 = differential operator
F = arbitrary function of vorticity defined in Equation (13)
f = function defined in Equation (40)
G = arbitrary function of vorticity defined in Equation (14)
h = lattice spacing, general
h = heat transfer coefficient
k = thermal conductivity
L = vortex length, dimensional
M = total number of division in grid, z direction
m = exponent of Prandtl number, Equation (31)
N = total number of division in grid, θ direction
n = exponent of Reynolds number, Equation (31)
N_{Nu} = overall Nusselt number, hD/k
P = coefficient defined in Equation (24)
p_0 = front stagnation pressure, dimensionless
N_{Pe} = Peclet number, $Pr \cdot Re$
N_{Pr} = Prandtl number, $c_p\mu/k$
Q = coefficient defined in Equation (24)
q = heat flux
R = radius of sphere
r = radial distance
r_∞ = distance from sphere surface to outer boundary, dimensionless
N_{Re} = Reynolds number, UD/ν
T = temperature
T' = dimensionless temperature (T/T_∞)
T_{fk} = dimensionless reference temperature for thermal conductivity
$T_{f\nu}$ = dimensionless reference temperature for kinematic viscosity
T_0 = ratio of temperature of sphere surface to that of the gas stream $= T_s/T_\infty$
$T_{0.19}$ = reference temperature defined in Equation (41), dimensional
U = free stream velocity
v = velocity vector component
W = relaxation coefficient
x = transport property exponent
z = dimensionless radial distance

Greek Letters

Γ = function defined in Equation (5)
Δ = difference
ζ = vorticity, ϕ component
θ = angle measured from front stagnation point
θ_s = separation angle, measured from near stagnation point

μ = viscosity
ν = kinematic viscosity
ρ = density
Σ = function defined in Equation (4)
Φ = arbitrary function
Ψ = stream function

Subscripts

f = evaluated at reference temperature
I = defining mesh point in θ direction
J = defining mesh point in z direction
r = in r direction
s = evaluated at surface conditions
θ = in θ direction
∞ = evaluated at free stream conditions

Superscript

$*$ = dimensionless variable

LITERATURE CITED

Acrivos, A., and T. D. Taylor, "Heat and Mass Transfer from Single Spheres in Stokes' Flow," *Phys. Fluids*, **5**, No. 4, 387 (1962).

Amdur, I., and A. E. Mason, "Properties of Gases at Very High Temperatures," *Phys. Fluids*, **1**, 370 (1958).

Baird, M. H., and A. E. Hamielec, "Forced Convection Transfer Around Spheres at Intermediate Reynolds Numbers," *Can. J. Chem. Eng.*, **40**, No. 3, 119 (1962).

Beard, K. V., and H. R. Pruppacher, "A Wind Tunnel Investigation of the Rate of Evaporation of Small Water Drops Falling at Terminal Velocity in Air," *J. Atmos. Sci.*, **28**, 1455 (1971).

Chester, W., and D. R. Breach, "On the Flow Past a Sphere at Low Reynolds Number," *J. Fluid Mech.*, **37**, No. 4, 751 (1969).

Clift, R., J. R. Grace, and M. E. Weber, *Bubbles, Drops and Particles*, Academic Press, New York (1978).

Dennis, S. C. R., and J. D. A. Walker, "Calculation of the Steady Flow Past a Sphere at Low and Moderate Reynolds Numbers," *J. Fluid Mech.*, **48**, No. 4, 771 (1971).

Dennis, S. C. R., J. D. A. Walker, and J. D. Hudson, "Heat Transfer from a Sphere at Low Reynolds Numbers," *ibid.*, **60**, No. 2, 273 (1973).

Drellishak, K. S., C. F. Knopp, and A. B. Cambel, "Partition Functions and Thermodynamic Properties of Argon Plasma," Arnold Engineering Development Centre, *Rept. No. AEDC, TDR63-146* (1963).

Dumargue, P., C. Bonet, and M. Daguenet, "Convective Evaporation of a Spherical Super-Refractory Particle Inside a Thermal Plasma: The Stokes' Problem in a Fluid with Variable Properties," Paper CT2.6 presented at the Fifth International Heat Transfer Conference, Tokyo, Japan (Sept. 3-7, 1974).

Griffith, R. M., "Mass Transfer from Drops and Bubbles," *Chem. Eng. Sci.*, **12**, 198 (1960).

Gupalo, Y. P., and Y. S. Ryazantsev, "Mass and Heat Transfer from a Sphere in a Laminar Flow," *ibid.*, **27**, 61 (1972).

Hamielec, A. E., and A. I. Johnson, "Viscous Flow Around Fluid Spheres at Intermediate Reynolds Numbers (I)," *Can. J. Chem. Eng.*, **40**, 41 (1962).

Hamielec, A. E., S. H. Storey, and J. M. Whitehead, "Viscous Flow Around Fluid Spheres at Intermediate Reynolds Numbers (II)," *ibid.*, **41**, 246 (1963).

Hamielec, A. E., T. W. Hoffman, and L. L. Ross, "Numerical Solution of the Navier-Stokes Equation for Flow Past Spheres," *AIChE J.*, **13**, No. 2, 212 (1967).

Hoffman, T. W., and L. L. Ross, "A Theoretical Investigation of the Effect of Mass Transfer on Heat Transfer to an Evaporating Droplet," *Int. J. Heat Mass Transfer*, **15**, 559 (1972).

Jenson, V. G., "Viscous Flow Round a Sphere at Low Reynolds Numbers (<40)," *Proc. Royal Soc. (London)*, **249A**, 346 (1959).

Kassoy, D. R., T. C. Adamson, and A. F. Messiter, "Compressible Low Reynolds Number Flow Around a Sphere," *Phys. Fluids*, **9**, No. 4, 671 (1966).

Kawaguti, M. J., "The Critical Reynolds Number for the Flow Past a Sphere," *J. Phys. Soc. Japan*, **10**, 694 (1955).

Kawaguti, M. J., "An Approximate Solution for the Slow Viscous Flow Around a Sphere," *ibid.*, **13**, 209 (1958).

Lapidus, L., *Digital Computation for Chemical Engineers*, McGraw-Hill, New York (1962).

LeClair, B. P., A. E. Hamielec, and H. R. Pruppacher, "A Numerical Study of the Drag on a Sphere at Low and Intermediate Reynolds Numbers," *J. Atmos. Sci.*, **27**, No. 2, 308 (1970).

LeClair, B. P., and A. E. Hamielec, "Flow Behaviour Around a Sphere Accelerating in a Viscous Fluid," Fluid Dynamics Symp., McMaster University, Hamilton, Ontario, Canada (Aug., 1970).

Oseen, C. W., "Ueber die Stokes' sche Formel, und über eine verwandte Aufgabe in der Hydrodynamik," *Ark. f. Mat. Astr. och Fys.*, **6**, No. 29 (1910).

Pei, D. C. T., C. Narasimhan, and W. H. Gauvin, "Evaporation from Drops and Particles in High-Temperature Surroundings," presented at Interaction Between Fluids and Particles Symposium, London, England (June, 1962).

Pei, D. C. T., "Heat Transfer from Spheres Under Combined Forced and Natural Convection," *Chem. Eng. Progr. Symposium Ser.*, **61**, No. 59, 57 (1965).

Proudman, I., and J. R. A. Pearson, "Expansions at Small Reynolds Numbers for the Flow Past a Sphere and a Circular Cylinder," *J. Fluid Mech.*, **2**, 237 (1957).

Pruppacher, H. R., B. P. LeClair, and A. E. Hamielec, "Some Relations Between Drag and Flow Pattern of Viscous Flow Past a Sphere and a Cylinder at Low and Intermediate Reynolds Numbers," *ibid.*, **44**, No. 4, 781 (1970).

Ranz, W. E., and W. R. Marshall, "Evaporation from Drops," *Chem. Eng. Progr.*, **48**, No. 3, 141 (1952).

Rimmer, P. L., "Heat Transfer from a Sphere in a Stream of Small Reynolds Number," *J. Fluid Mech.*, **32**, No. 1, I (1968).

Rimon, Y., and S. I. Cheng, "Numerical Solution of a Uniform Flow Over a Sphere at Intermediate Reynolds Numbers," *Phys. Fluids*, **12**, No. 5, 949 (1969).

Roache, P. J., *Computational Fluid Dynamics*, Hermosa Publ., Albuquerque, N. Mex. (1972).

Roos, F. W., and W. W. Willmarth, "Some Experimental Results on Sphere and Disk Drag," *AIAA Journal*, **9**, No. 2, 285 (1971).

Sayegh, N. N., "Variable Property Flow and Heat Transfer to Single Spheres in High Temperature Surroundings," Ph.D. thesis, Department of Chemical Engineering, McGill Univ., Montreal, Quebec, Canada (1977).

Seymour, E. V., "The Hydrodynamic Drag on a Small Sphere in an Ionized Gas," *Trans. ASME J. Appl. Mech.*, **93**, 739 (1971).

Stokes, C. G., "On the Effect of the Internal Friction of Fluids on the Motion of Pendulums," *Trans. Camb. Phil. Soc.*, **9**, 8 (1950).

Taneda, S., "Experimental Investigation of the Wake Behind a Sphere at Low Reynolds Numbers," *J. Phys. Soc. Japan*, **11**, 1104 (1956).

Whitaker, S., "Forced Convection Heat Transfer Correlations for Flow in Pipes, Past Flat Plates, Single Cylinders, Single Spheres, and for Flow in Packed Beds and Tube Bundles," *AIChE J.*, **18**, No. 21, 361 (1972).

Woo, S. E., Ph.D. thesis, McMaster Univ., Hamilton, Canada (1970).

———, and A. E. Hamielec, "A Numerical Method of Determining the Rate of Evaporation of Small Water Drops Falling at Terminal Velocity in Air," *J. Atmos. Sci.*, **28**, No. 8, 1448 (1971).

Yuan, S. W., *Foundations of Fluid Mechanics*, Prentice Hall, Englewood Cliffs, N.J. (1967).

Manuscript received October 17, 1978; revision received February 15, and accepted February 20, 1979.